

PORTAL FRAMES WITH I-BEAM TO RHS-COLUMN JOINTS

Daniel J. R. Pereira¹

drocha044@gmail.com

João B. S. Neto¹

joaobatista011@gmail.com

Matheus M. Oliveira¹

matheusmoliveira4@gmail.com

Messias J. L. Guerra²

messias.guerra@ifmg.edu.br

Gabriel V. Nunes³

gabriel.nunes@ifmg.edu.br

Arlene M. C. Sarmanho¹

arlene.sarmanho@gmail.com

¹*Universidade Federal de Ouro Preto*

Departamento de Engenharia Civil – Campus Universitário Morro do Cruzeiro, Ouro Preto, 35400-000/MG, Brasil.

²*Instituto Federal de Minas Gerais – Campus Santa Luzia.*

³*Instituto Federal de Minas Gerais – Campus Congonhas.*

Abstract. This paper analyses welded joints in portal frames with I-beams and rectangular hollow section columns. The study of joints is essential to the understanding of the structural behavior of portal frames, and the analysis of its stiffness enables a better understanding of moment transmission between tubular columns and I-beams, besides enabling the joint classification. Through numerical analysis using a commercial software, the representation of the models was implemented in finite elements, with subsequent displacement simulation. The slenderness of the tubular columns and the beam-to-column width ratio were varied. The moment-rotation curves for each joint in a portal frame were presented, and the influence of the parameters involved was presented graphically, where it was possible to visualize yielding in some regions. Plastification of the column face occurred in the cases, while all connections were classified as semi-rigid. Arrangements with different beam lengths were made, where it was possible to observe its influence on the joint classification.

Keywords: Tubular joints, steel structures, initial stiffness.

1 Introduction

This paper aims to evaluate welded joints in portal frames with rectangular hollow section (RHS) columns and I-beams through a numerical analysis via commercial software.

Previous studies were performed in this arrangement with a single [1], [2] and two beams [3], [4], where equations were proposed to quantify the connections' rigidity.

The current national normative prescriptions [5], [6] do not contemplate the design of joints that are not considered rigid or pinned.

Rigid joints allow a full continuity analysis, while nominally pinned joints do not transmit significant bending moments through the components. An intermediate case are the semi-rigid joints, which present an in-between behavior between rigid and pinned, as given by EN 1993-1-8 [7].

Studies show that most joints could behave as semi-rigid [8]–[10], and it is possible to quantify the stiffness and resistance of these joints to provide lighter and more economical designs.

Therefore, 15 numerical models with different with geometric properties were analyzed. A study of the beam length with 5 models was also undertaken, aiming to evaluate its influence on the joint behavior.

2 Theoretical review

To evaluate a joint, the geometric parameters and proper rigidity classification are necessary. The parameters adopted and its nomenclature are currently used in normative prescriptions [7], enabling a better understanding of the connection behavior.

2.1 Geometric parameters

The geometric parameters for the joint analysis are shown in Figure 1, where the ratios β and 2γ are used to quantify the proportion between the beam and column widths and the column slenderness, respectively.

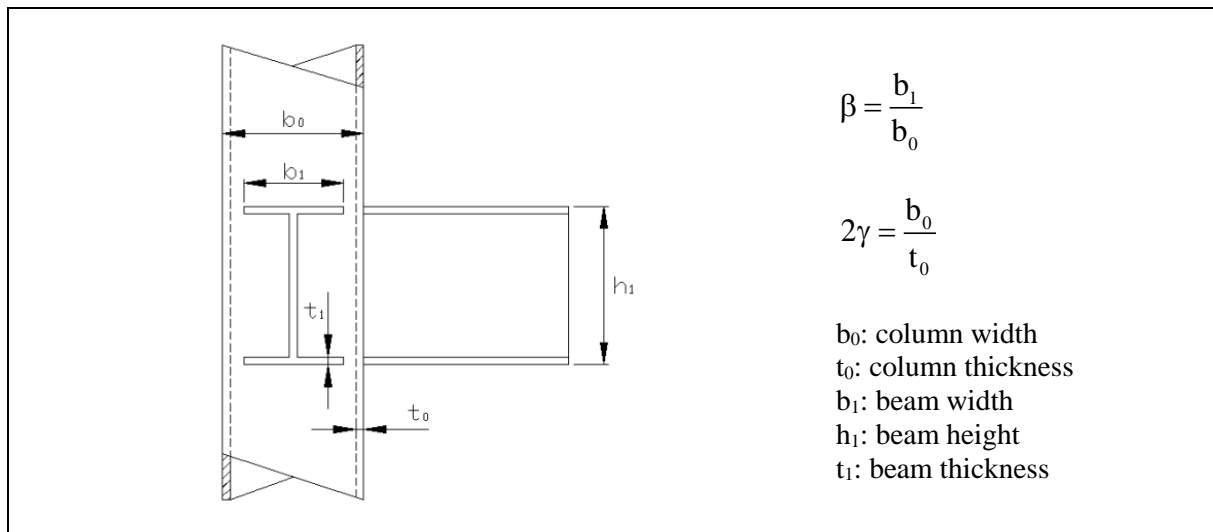


Figure 1. Geometric parameters.

2.2 Joint classification

A joint can be classified as rigid, nominally pinned or semi-rigid, according to the limits prescribed by EN 1993-1-8 [7], as shown in Figure 2.

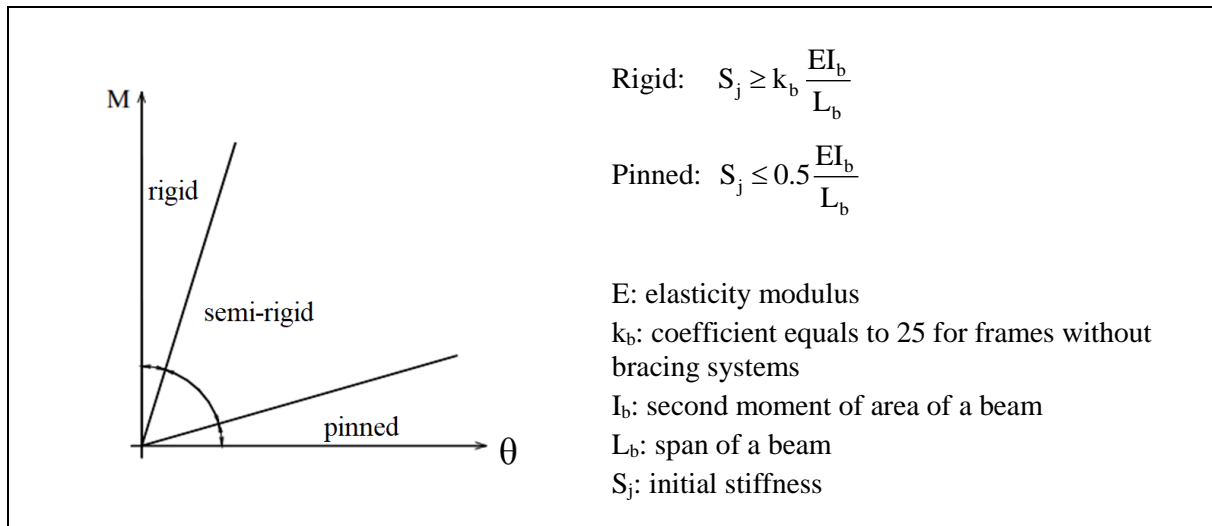


Figure 2. Classification of joints by stiffness according to EN 1993-1-8 [7].

3 FE analysis

3.1 Parametric study

In the parametric study, 15 models with 2m long beams and 1m long columns were chosen, with variations of the column's thickness and the beam's width, which are shown in Table 1.

Table 1. Parametric study with a 2m long beam.

Model	Column			Beam				Parameters	
	h ₀ [mm]	b ₀ [mm]	t ₀ [mm]	h ₁ [mm]	b ₁ [mm]	t ₁ [mm]	L [m]	β	2γ
1					60			0.40	
2					75			0.50	
3	150	150	3.0	200	90	3.0	2.0	0.60	50.0
4					105			0.70	
5					120			0.80	
6					60			0.40	
7					75			0.50	
8	150	150	4.0	200	90	4.0	2.0	0.60	37.5
9					105			0.70	
10					120			0.80	
11					60			0.40	
12					75			0.50	
13	150	150	6.0	200	90	6.0	2.0	0.60	25.0
14					105			0.70	
15					120			0.80	

The choice of parameters to vary were made considering the analyses of the columns' slenderness (2γ) and the beam-to-column width ratio (β), with adequate proportions for execution. Furthermore, the beam length variation was also considered in additional models, from lengths from 2 to 6m, as described in Table 2.

Table 2. Models with different beam lengths.

Model	Column			Beam				Parameters	
	h_0 [mm]	b_0 [mm]	t_0 [mm]	h_1 [mm]	b_1 [mm]	t_1 [mm]	L [m]	β	2γ
16							2.0		
17							3.0		
18	150	150	3.0	200	60	3.0	4.0	0.40	50.0
19							5.0		
20							6.0		

3.2 Material properties

Non-linear geometrical and material analysis were undertaken to study the joint behavior. The steel properties used were a 345MPa yield strength, 450MPa ultimate strength and 200GPa elasticity modulus.

3.3 Numerical modeling

The numerical modeling was made in the finite element (FE) software Ansys [11], using the element SHELL 281, that provides eight nodes with six degrees of freedom each.

A bilinear diagram was used to simulate the material performance, considering a tangent modulus with a 10% of the elasticity modulus value. The geometric parameters simulation included a fillet weld with 1.5 times the column thickness (t_0) leg size, as shown in detail in an isolated joint in Figure 3.

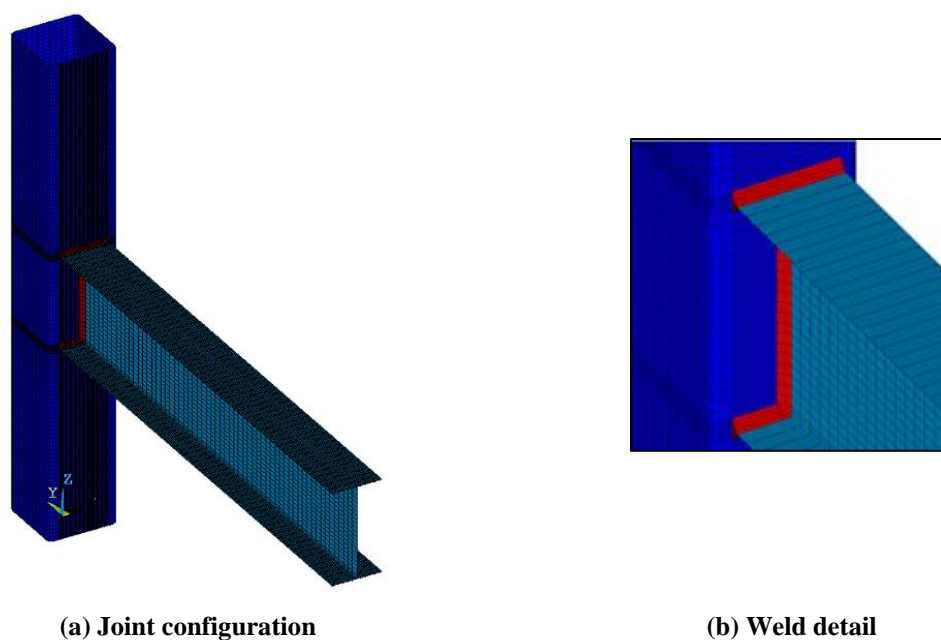


Figure 3. Mesh details.

Different mesh configurations were tested in isolated joints with the geometric properties of Model 6, described in Table 1. A coarse mesh did not affect the results of the initial behavior of the joint; however, different results were observed after the linear part of the curve – Figure 4, leading to the adoption of the fine mesh in all analyses.

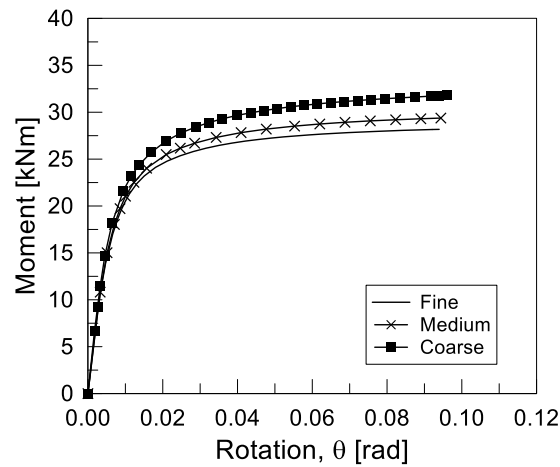


Figure 4. Moment-rotation behavior under different mesh sizes.

Furthermore, the mesh adopted, shown in Figure 5, is finer in the joint region, where stress concentrations are expected. The corner radius was considered 1.5 times the column thickness, as recommended by EN 10219-2 [12]. Displacements at the center of the beam were applied, simulating a compressive loading situation. The nodes at the ends of columns and regions of displacement appliance – center of the beam – were coupled to distribute the boundary or displacement conditions to the other nodes at the section. A Newton-Raphson iterative method was chosen as the system of equations solution.

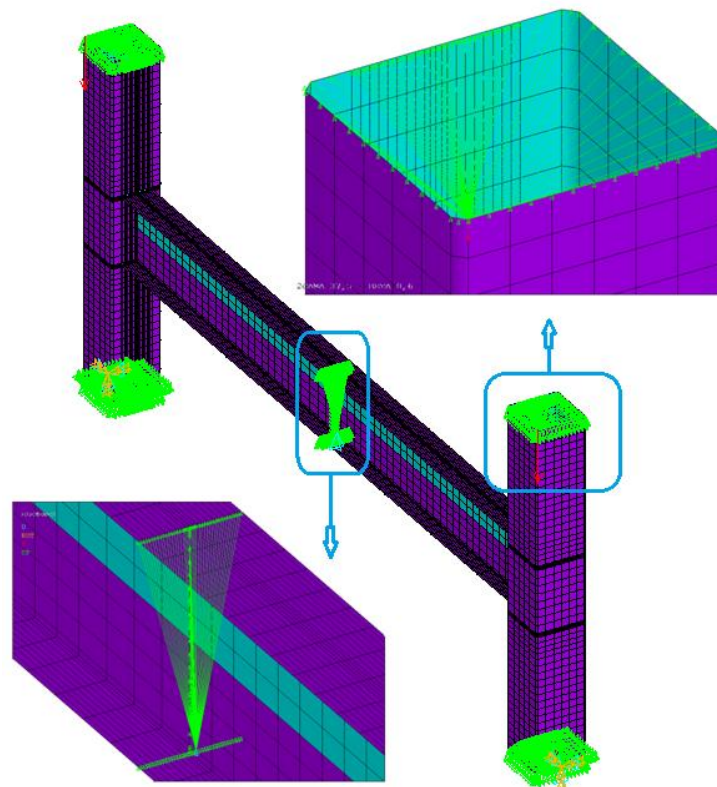


Figure 5. Portal frame in the FE modeling.

4 Results and discussion

4.1 Joint behavior

With the presence of bending moment in a beam in the RHS-column and I-beam joint configuration, the column face plastification is a possible failure mode – the column face is usually subjected to compression in the lower part and tension in the upper, as shown in Figure 6.

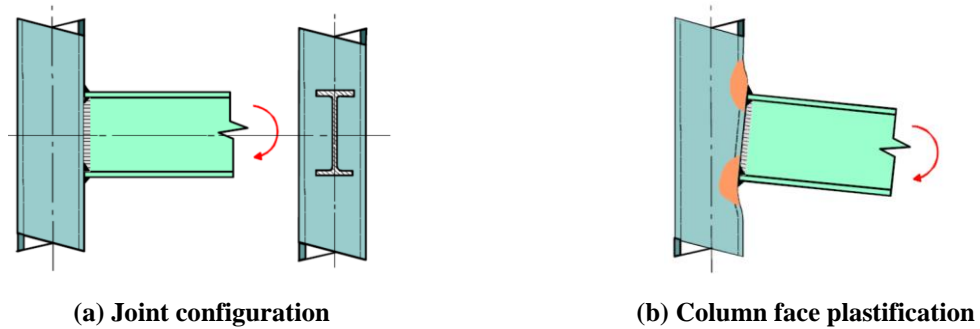


Figure 6. Joint configuration and possible failure mode [13].

For the models described in Table 1, the Moment-rotation behavior of the joints is shown in Figure 7. The clear influence of the parameters β and 2γ on the joint behavior is can be observed.

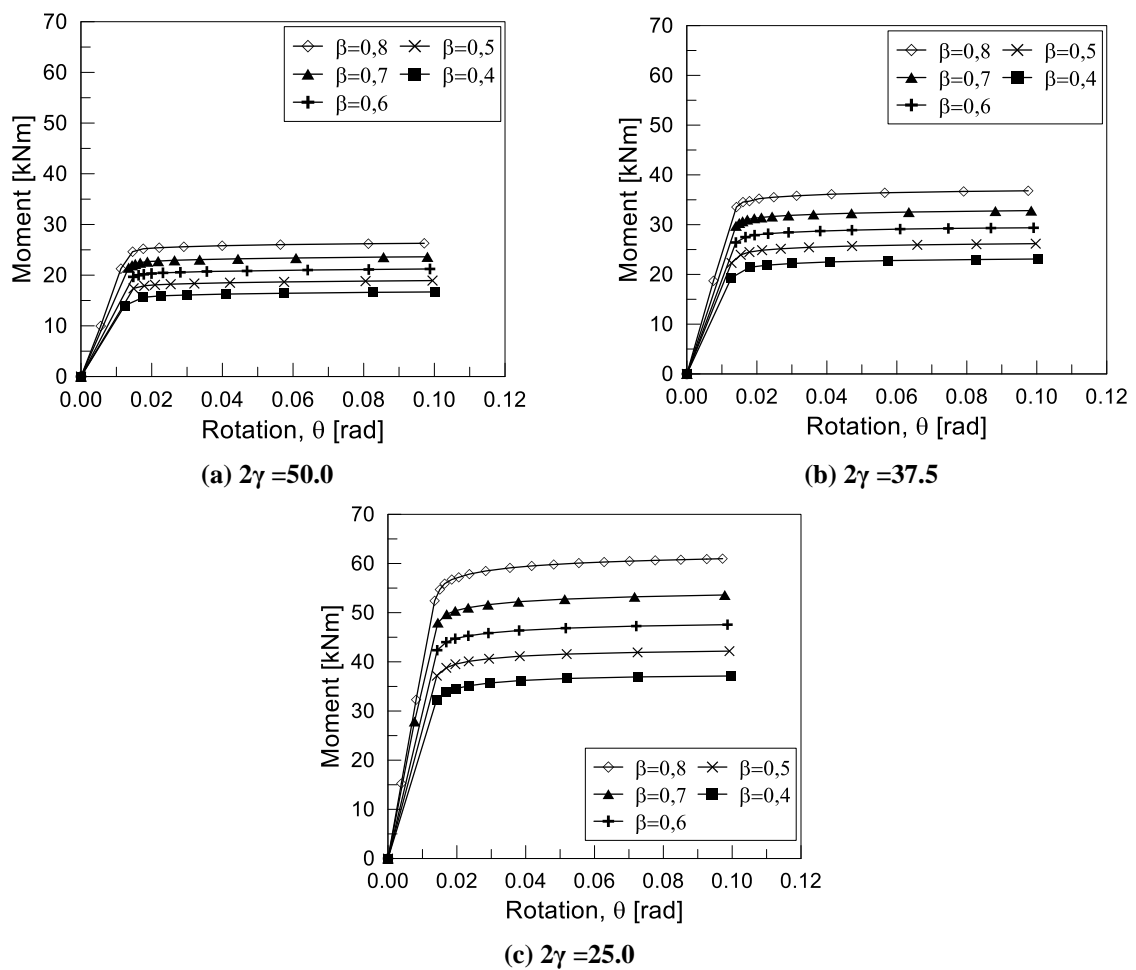


Figure 7. Moment-rotation behavior.

4.2 Joint classification

The initial stiffness (S_j) results for the models are presented in Table 3, as the upper ($S_{j,sup}$) and lower ($S_{j,inf}$) classification limits. All models can be classified as semi-rigid.

Table 3. Initial stiffness results.

Model	$\beta/2\gamma$	Classification Limits		Results	
		$S_{j,sup}$ [kNm/rad]	$S_{j,inf}$ [kNm/rad]	S_j [kNm/rad]	$S_j / (E t_0)$
1	0.008	14272.7	285.5	1133.3	0.00189
2	0.010	16590.9	331.8	1171.7	0.00195
3	0.012	18909.1	378.2	1330.9	0.00222
4	0.014	21227.2	424.5	1593.7	0.00266
5	0.016	23545.4	470.9	1788.1	0.00298
6	0.011	19153.1	383.1	1520.0	0.00190
7	0.013	22274.7	445.5	1748.2	0.00219
8	0.016	25396.3	507.9	1887.8	0.00236
9	0.019	28517.9	570.4	2122.3	0.00265
10	0.021	31639.5	632.8	2463.8	0.00308
11	0.016	29101.6	582.0	2288.5	0.00191
12	0,020	33877.0	677.5	2620.6	0.00218
13	0.024	38652.4	773.0	2963.5	0.00247
14	0.028	43427.8	868.6	3611.0	0.00301
15	0.032	48203.2	964.1	3937.8	0.00323

4.3 von Mises stresses

The von Mises stresses distribution for models with β equals to 0.40 and 0.80 are exposed in Figure 8, in different steps of loading. It is observed the formation of plastic hinges at the center of the beams at higher displacement levels, as the concentration of stresses at the joint region.

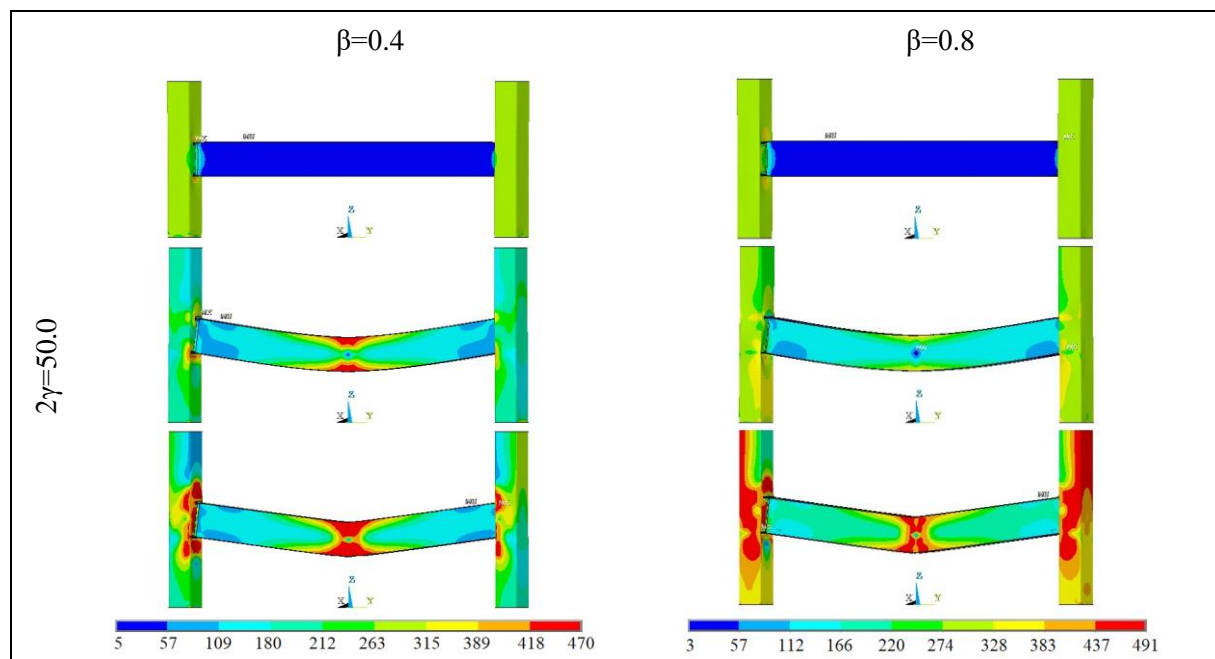


Figure 8. von Mises stresses distribution [MPa] (Continues).

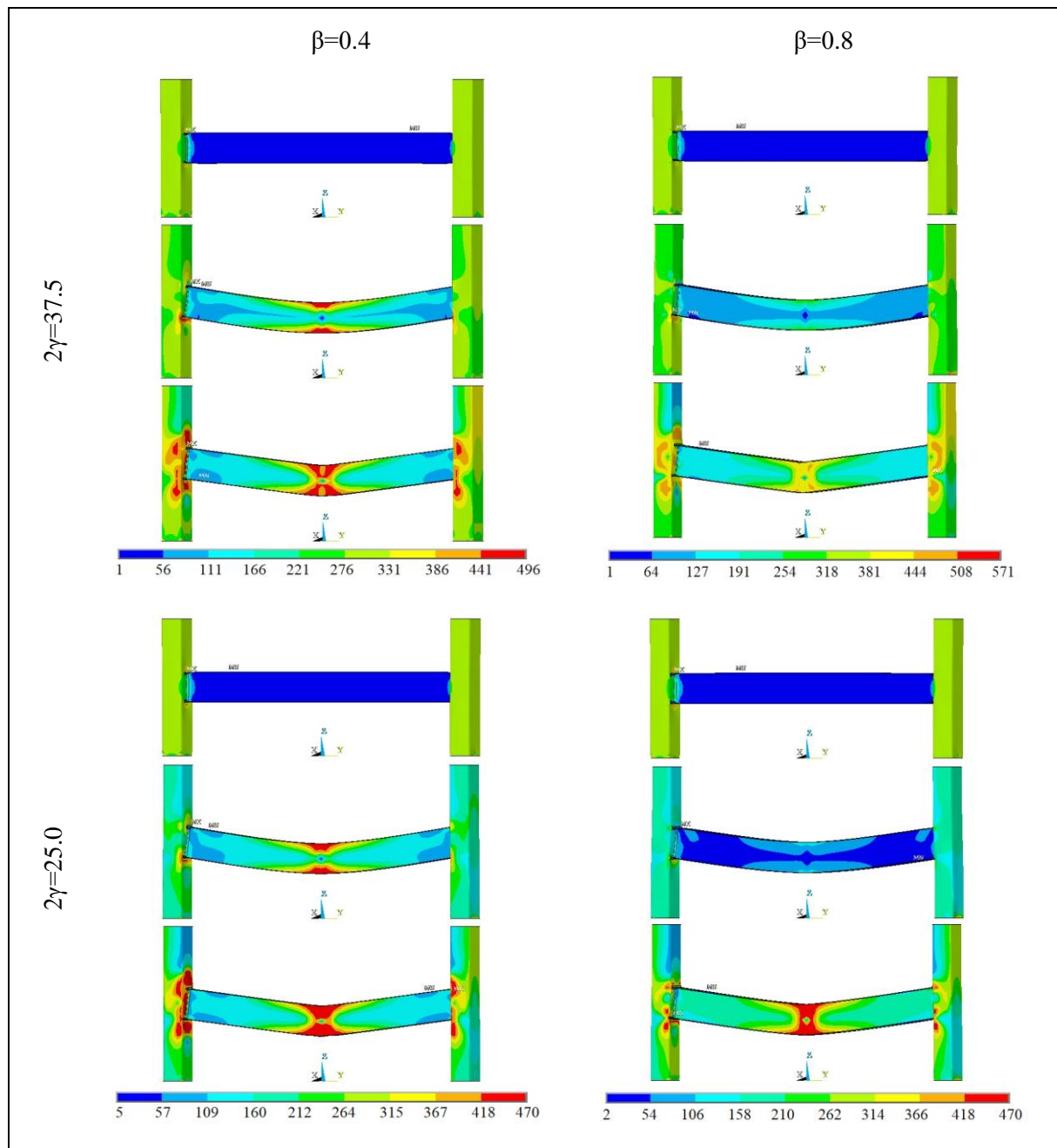


Figure 8. von Mises stresses distribution [MPa] (End).

4.4 Beam length variation

The influence of the beam length on the rigidity of a joint was analyzed in a frame with $2\gamma=50$ e $\beta=0.4$ with the properties of Model 1 (Table 1), and the Moment-Rotation behavior shown in Figure 9. All joints were classified as semi-rigid, even though the 5m and 6m beams almost reached a flexible definition, according to the described limits.

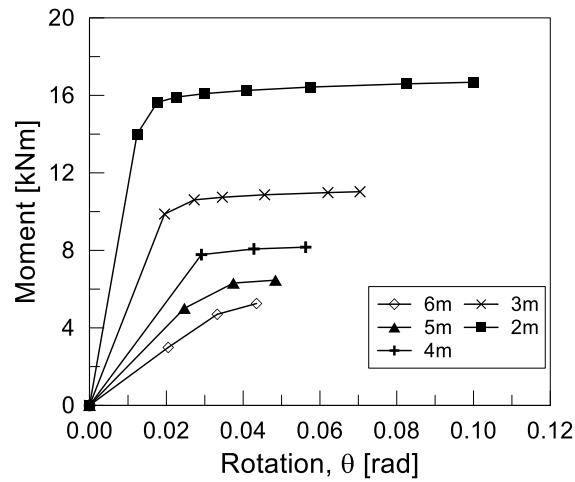


Figure 9. Joint behavior under different beam lengths for $2\gamma=50$ and $\beta=0.40$.

The initial stiffness results for each of the models are shown in Table 4. The classification of the models was all semi-rigid.

Table 4. Initial stiffness for different beam lengths.

S_j [kNm/rad]	Beam length				
	2m	3m	4m	5m	6m
$S_{j,sup}$	14272.7	9515.1	7136.4	5709.1	4757.6
$S_{j,inf}$	285.5	255.4	191.5	153.2	127.7
S_j	1133.3	505.9	267.1	202.9	146.1

5 Results comparison

Previous studies of this type of joint considering one column connected to on beam [1] and two beams [3] are compared to the current frame analysis in Figure 10, with a $2\gamma=25$, $\beta=0.40$ and 1m long beam configuration, considering the same material parameters of Model 1 (Table 1) and same numerical method. The influence of the geometry set is observed, where the frame presented a higher rigidity than the other configurations.

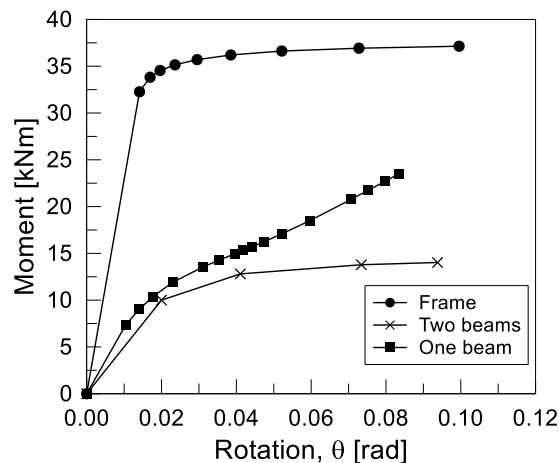


Figure 10. Joint behavior comparison.

The Equations 1 and 2, proposed by previous works analyzing isolated joints [1], [3], are presented.

$$S_j = 3.0Et_0 \left[\frac{\beta}{2\gamma} \right]^{2.0} \quad \text{one beam configuration} \quad (1)$$

$$S_j = 6.4Et_0 \left[\frac{\beta}{2\gamma} \right]^{2.3} \quad \text{two beams configuration} \quad (2)$$

Using Equation 1, the rigidity of the joint is equivalent to 115.2 kNm/rad. Therefore, it does not represent well the behavior of joints inside the portal frames analyzed in this paper. As it was observed in Figure 9, the beam length in a portal frame is decisive in a joint behavior. The equations do not contemplate this variable, and, therefore, a further analysis is necessary to englobe the calculation of the rigidity of the type of joint studied.

6 Final considerations

The numerical analysis with finite elements provided a proper simulation of RHS-column to I-beam joints inside a portal frame configuration, with a precise portrait of the plastification of the column face and the formation of plastic hinges.

The 15 joints analyzed – slenderness values of 25.0, 37.50 and 50.0 and with beam-to-column width ratios varying from 0.40 to 0.80 – were all classified as semi-rigid.

With higher beam-to-column width ratios, higher values of joint resistance were found. Plastification of the column face was the dominant failure mode encountered.

The beam length was shown to be determinant in the joint behavior.

Equations to determine the RHS-column to I-beam joint rigidity proposed by other papers showed a discrepancy with the analysis of portal frames, and further studies are necessary to accommodate variables not currently considered.

Acknowledgements

The authors thank Universidade Federal de Ouro Preto (UFOP), CAPES, FAPEMIG, CNPq and IFMG for the financial support.

References

- [1] M. J. L. Guerra, S. L. Ferrarezi, G. V. Nunes, and A. M. C. Sarmanho, “Análise de ligações metálicas soldadas entre pilar de seção RHS e viga de seção I,” in *Proceedings of the XXXIV Iberian Latin-American Congress on Computational Methods in Engineering*, 2013.
- [2] B. S. Rocha and J. G. R. Neto, “Análise de ligações soldadas entre vigas de seção I e pilares em perfis tubulares,” in *Proceedings of the XXXVII Iberian Latin-American Congress on Computational Methods in Engineering*, 2016.
- [3] D. J. R. Pereira, M. J. L. Guerra, T. H. S. Santos, G. v. Nunes, and A. M. C. Sarmanho, “Estudo da rigidez em ligações entre perfis de aço de seção tubular retangular e perfis I,” in *Construmetal 2019 – 8º Congresso Latino-americano da Construção Metálica*, 2019.
- [4] T. C. Nunes, A. M. Sarmanho, G. D. de Paula, and M. S. R. Freitas, “Análise de ligações metálicas soldadas entre pilar de seção RHS e viga de seção I,” *Rev. da Estrut. Aço - REA*, vol. 1, no. 3, pp. 167–180, 2012.
- [5] NBR 16239, *Projeto de estruturas de aço e de estruturas mistas de aço e concreto de edificações com perfis tubulares*, 1st ed. Rio de Janeiro: Associação Brasileira de Normas Técnicas, 2013.

- [6] NBR 8800, *Projeto de estruturas de aço e de estruturas mistas de aço e concreto de edifícios*. Rio de Janeiro: Associação Brasileira de Normas Técnicas, 2008.
- [7] EN 1993-1-8, *Eurocode 3: Design of steel structures. Part 1-8: Design of joints*. Brussels: CEN (European Committee for Standardization), 2005.
- [8] A. T. Silva, A. M. C. Sarmanho, G. V. Nunes, D. J. R. Pereira, and L. H. de A. Neiva, “Cold formed steel semi rigid joints,” *REM - Int. Eng. J.*, vol. 71, no. 4, pp. 497–504, Dec. 2018.
- [9] L. R. O. de Lima, L. Simões da Silva, P. C. G. d. S. Vellasco, and S. A. L. de Andrade, “Experimental evaluation of extended endplate beam-to-column joints subjected to bending and axial force,” *Eng. Struct.*, vol. 26, no. 10, pp. 1333–1347, Aug. 2004.
- [10] V. Gomes, A. T. Silva, L. R. O. de Lima, and P. C. G. da S. Vellasco, “Numerical investigation of semi-rigid connection ultimate capacity,” *REM - Int. Eng. J.*, vol. 71, no. 4, pp. 505–512, Dec. 2018.
- [11] ANSYS Inc., “ANSYS Versão 12.0.” .EUA, 2012.
- [12] EN 10219-2, *Cold formed welded structural hollow sections of non-alloy and fine grain steels - Part 2: Tolerances, dimensions and sectional properties*. Brussels: CEN (European Committee for Standardization), 2006.
- [13] J. Wardenier, J. A. Packer, X.-L. Zhao, and G. J. van der Vegte, *Hollow sections in structural applications*. Geneva: CIDECT, 2010.